Strange Anti-particle to particle ratios at mid-rapidity in $\sqrt{s_{NN}} = 130$ GeV Au+Au Collisions.

(September 7, 2001)

Official author list will be inserted.

Abstract

Results on the anti-particle to particle ratios of the mid-rapidity yields of Λ, Ξ and charged kaons are reported, as measured in $\sqrt{s_{NN}} = 130$ GeV Au+Au collisions using the STAR detector system. We obtain values of $\overline{\Lambda}/\Lambda = 0.69 \pm 0.01(stat.)$, $\overline{\Xi}^{+}/\Xi^{-} = 0.87 \pm 0.04(stat.)$ and $K^{+}/K^{-} = 1.083 \pm 0.008(stat.)$. The ratios indicate that the mid-rapidity region is not net baryon free and that the excess of baryons in the initial system is also present in the mid-rapidity hyperons. We note that the trend in the progression of the baryon ratios, with increasing strange quark content, is similar to that observed in heavy-ion collisions at lower energies. The value of these ratios can be simply related to the charged kaon ratio in the framework of a simple quark-counting model.

The goal of the experimental program at the Relativistic Heavy Ion Collider (RHIC) is to study the new states of nuclear matter which have been predicted to form in heavy-ion collisions [1] and for which some evidence has emerged from a previous series of experiments at lower energy [2]. Measurements of anti-particle to particle ratios in such collisions give information on the net baryon density or baryochemical potential achieved [3] and are thus of interest in characterizing the environment created in these collisions. It has also been suggested that the strange anti-baryon to baryon ratios may be enhanced in a quark-gluon plasma [4]. This is a consequence of the predicted enhancement of strange quark-antiquark pair production in the plasma state [5,6], resulting in a stronger enhancement of strange antibaryons over strange baryons compared to purely hadronic interactions.

The Solenoidal Tracker at RHIC (STAR) detector system [7], in the configuration used to collect the data presented here, consisted principally of a large cylindrical Time Projection Chamber (TPC) used for charged particle tracking. The TPC has inner and outer radii of 50 cm and 200 cm, a total length of approximately 400 cm and was operated in a 0.25 Tesla magnetic field. It was surrounded by a cylinder of 240 scintillator slats forming a Central Trigger Barrel (CTB). Two Zero Degree Calorimeters (ZDCs), situated 18m East and West of the center of the TPC were used to detect spectator neutrons from the colliding ions at close to beam rapidities. Collisions were triggered by requiring coincident signals in the ZDCs which formed a minimum bias trigger. An enriched central data sample, was acquired with the additional requirement of a high CTB threshold, corresponding approximately to the 14% most central events. A further centrality selection was made offline, by cutting on the observed track multiplicity in the TPC after event reconstruction. The data used in this analysis were 180,000 central events after the multiplicity cut, which selected the top 11% of the measured cross-section [8].

Two types of technique have been used to extract the raw yields of strange particles. Firstly, charged kaons were identified via their specific ionization, or energy loss (dE/dx), in the TPC. Secondly, these and other strange particles were reconstructed from the topology of their daughters following weak decay.

The dE/dx method for identifying charged kaons is only applicable below a momentum of 0.6 GeV/c, where the energy loss of kaons is distinct from that of pions within our resolution. Tracks were selected on the basis that they originate from the primary interaction vertex. Each track may contain up to 45 measurements of the ionization along its length. A 75% truncation was applied to the measured dE/dx samples [10] in order to reduce the effect of fluctuations in the ionization distribution. The resulting mean dE/dx for each track was divided by the energy loss calculated for a kaon with the same momentum from the Bethe-

Bloch equation. When the logarithm of this ratio, $Z = log[(dE/dx)_{Meas}/(dE/dx)_{BB}]$, is plotted, Gaussian-like peaks are obtained for pions, electrons, kaons and protons. Fitting the distribution with a convolution of Gaussian functions allows the yield of each particle to be determined, that of kaons being the integral of the Gaussian centered closest to zero. This procedure was undertaken as a function of the p_T and rapidity of the kaon. Distributions in the Z variable are shown in Figure 1 for both positive and negative particles and for bins at either end of the range of the measurement which is 0.15 GeV to 0.6 GeV/c in p_T.

The most versatile technique for the reconstruction of strange particles is via their decay topologies. The decay $\Lambda \rightarrow p\pi^-$ and the charge conjugate decay for $\overline{\Lambda}$ results in two charged particles in the final state and has a 64% branching ratio. The Λ particles from the electromagnetic decay of the Σ^0 are included in the Λ sample since they are indistinguishable from the primary Λ population. The momentum of these charged daughter particles is measured from their curvature in the TPC. Both tracks can be extrapolated back toward the primary interaction vertex to locate their common point of origin, from which the kinematic properties of the parent can be calculated. In the process of reconstruction all pairs of positively and negatively charged tracks in an event are considered. A selection must be made to reduce the large combinatorial background which results from random crossings of tracks interior to the TPC fiducial volume. The most important criteria for improving the signal to noise ratio are that the decay vertex is well separated from the primary interaction and that the parent originates from the primary interaction vertex but that the daughters do not. An additional requirement that the dE/dx of the daughters is compatible with the expected decay mode is also applied. The small remaining background within ± 15 MeV/c^2 of the peaks in the invariant mass distributions of Figure 2 was subtracted by using a linear interpolation between the background regions on either side of the mass peaks. This technique is extended to enable the reconstruction of the $\Xi^- \rightarrow \Lambda\pi^-$ decay and the charge conjugate $\overline{\Xi}^+$ decay, which has a 100% branching ratio. Here, only Λ (or $\overline{\Lambda}$) candidates within ± 7 MeV/c^2 of the expected mass [11] are used and the requirement that the Λ (or $\overline{\Lambda}$) originates from the primary interaction vertex is relaxed. The resulting invariant mass distributions for Λ and Ξ^- with their anti-particle distributions superimposed are shown in Figure 2.

Charged kaons can also be reconstructed using a variation on this topological technique via the $K \rightarrow \mu\nu$,$K \rightarrow \pi\pi^0$, which have a 64% and 21% branching ratios, and other one-prong decay channels. In this "kink" method the tracks from the charged kaon and charged daughter particle are used to reconstruct the kinematics of the decay. The background comes from charged pion decays, multiple scattering and hadronic interactions in the TPC gas plus purely combinatoric background. Studies showed that the background level was approximately 15%. The pion decay contribution can be eliminated by applying a cut on the opening angle between the parent and daughter tracks, due to the smaller Q-value of the pion decay and lighter mass of the pion. In order that both parent and daughter are reconstructed in the TPC with good momentum resolution, the fiducial volume for the location of the decay vertex is restricted. This reduces the number of kaons reconstructed by this method to approximately five per central event and typically only one or two survive the offline cuts. In contrast several tens per event can be identified by the dE/dx method. The decay vertex restriction does not in itself introduce any restriction on p_T, allowing charged kaons to be measured out to 2 GeV/c in p_T beyond which the statistical error on the sample from this dataset becomes large.

The central assumption in forming the antiparticle to particle ratios is that the detector is symmetric to charge and therefore no corrections to the yields for the reconstruction efficiency or detector acceptance are required. However, losses due to the absorption of anti-protons in the detector material and feed-down from the decay of heavier strange baryons have the potential to modify both the $\overline{\Lambda}/\Lambda$ and $\overline{\Xi}^+/\Xi^-$ratios. We do not address the modification of the ratios by processes such as annhilation in the collision zone before freezeout as these are independent of the experimental setup and method.

Absorption causes the final state anti-proton from $\overline{\Lambda}$ decay to fail to be reconstructed more often than the proton from Λ decay. The size of this effect has been estimated and corrected for using a GEANT simulation of the detector. The absorption correction is found to cause the apparent $\overline{\Lambda}/\Lambda$ and $\overline{\Xi}^{+}/\Xi^{-}$ ratios to be x% and y% smaller that the actual ratios. The reported numbers have been corrected for this effect. In principle, the decaying anti-particles themselves also have a larger absorption cross-section than their corresponding particles but since they decay after only a few centimetres, before the dominant absorbing materials have been traversed, this has a negligible effect on the ratios and is included in the previous correction.

The composition of particles produced in the collision can by itself affect the observed $\overline{\Lambda}/\Lambda$ via feed-down from the decays of heavier strange particles. The feed-down contribution to the Λ originates from Ξ^{-}, Ξ^{0} and Ω^{-} decays. Only the dominant contribution from Ξ^{-} and Ξ^{0} have been considered. This was done by simulating events containing Λ and charged Ξ in the ratio indicated by preliminary STAR results and further assuming the Ξ^{0} are equal to Ξ^{-}. The resulting feed-down correction to the $\overline{\Lambda}/\Lambda$ is estimated to be in the range $4-6\%$. The only feed-down contribution to the $\overline{\Xi}^{+}/\Xi^{-}$ comes from the $\Omega^{-} \rightarrow \Xi^{-}\pi^{0}$ channel with a 9% branching fraction and this has been neglected.

The main contribution of non-primary K^{+} and K^{-} comes not from feed-down but from interactions of the produced particles within the detector material. The modification of the K^{+}/K^{-} due to the secondary interactions has been studied using GEANT simulations of HIJING [12] events and was found to be in the region of 1%.

After the absorption correction, the value of the $\overline{\Lambda}/\Lambda$ ratio is $0.73 \pm 0.03(stat.)$ in the measured acceptance interval of $p_T > 0.4$ GeV/c and within one unit of rapidity centered at mid-rapidity. The $\overline{\Xi}^{+}/\Xi^{-}$ ratio after correction is $0.87 \pm 0.03(stat.)$, measured over the same rapidity interval and $p_T > 0.5$ GeV/c. Both ratios are found to be constant to within $\pm y$% as a function of rapidity and p_T out to 2.5 GeV/c. The ratio is also flat as a function of the mid-rapidity charged particle multiplicity to within 3%.

The K^{+}/K^{-}ratio is $1.083 \pm 0.008(stat.)$ measured in the range $0.15 < p_T < 0.6$ GeV/c and ± 0.4 units of rapidity around mid-rapidity. The same ratio measured by the kink method is approximately $1.14 \pm 0.015(stat.)$ and extends out to 2 GeV/c in p_T. The ratio measured via both methods shows no significant deviation from a constant as a function of p_T. The systematic error of the kink measurement due to detector effects is estimated to be 0.05 and that for the dE/dx is estimated at 0.03. This small disagreement between the two methods is within the estimated systematic errors.

The strange anti-baryon to baryon ratios have been plotted in Figure 3 together with their values found in Pb+Pb collisions at $\sqrt{s_{NN}}$ = 17 GeV [13] measured at the CERN SPS. Also shown are the $\overline{p}/p$ ratios from STAR [14] and two measurements at the lower energy from NA44 [15] and NA49 [16]. The STAR measurement is taken for the 11% most central events to be consistent with the data presented here. It can be seen from Figure 3 that the ratios increase with increasing strangeness content of the baryon at both $\sqrt{s_{NN}}$ = 17 GeV and $\sqrt{s_{NN}}$ = 130 GeV. The close to linear trend between the ratios finds a possible explanation in terms of a simple quark coalescence model [17,18], which predicts that the antibaryon to baryon ratios should be related to one another by a common multiplicative factor. The multiplicative factor turns out to be the value given by the K^+/K^- ratio. This is in approximate agreement with the data presented here, as shown in Table I. However, the coalescence model presupposes that hadrons are formed from a system of independent quarks and anti-quarks. An alternative description of particle production is a statistical model approach [19], which does not distinguish between quark or hadron degrees of freedom. In this case the multiplicative factor is $\lambda \approx exp(2\mu_B/3T)$, where μ_B is the baryon chemical potential and T is the (chemical freeze-out) temperature. The K^+/K^- ratio can therefore be seen to be an indirect measure of the baryon chemical potential. If the central region in Au+Au collisions at $\sqrt{s_{NN}}$ = 130 GeV were net baryon free ($\mu_B = 0$), then the K^+/K^- ratio would be equal to unity, and in both models the antibaryon to baryon ratios would also be equal to unity, under the assumption that strangeness is locally conserved. However, while the anti-baryon to baryon ratios at this higher energy are closer to unity, reflecting a lower net-baryon density, the net-baryon density is nevertheless still finite. This is a consequence of baryon number transport (or stopping) during the collision process, such that there is an excess of light (up and down) quarks over antiquarks that favours the production of baryons over antibaryons and K^+ over K^-. If the chemical freeze-out temperature of $T = 168$ MeV obtained from a statistical model analysis [20] of the lower energy data is only weakly dependent on the baryon chemical potential, which is to be expected, then we find that $\mu_B \approx 35 - 50$ MeV at $\sqrt{s_{NN}} = 130$ GeV, in the temperature range 170-200 MeV, compared to $\mu_B = 266$ MeV at $\sqrt{s_{NN}} = 17$ GeV.

In summary, we have reported on strange anti-particle to particle ratios measured by the STAR experiment at mid-rapidity in the 11% most central Au+Au collisions at $\sqrt{s_{NN}}$ = 130 GeV. The ratios are consistent with simple quark counting models and with a statistical description of particle production which is governed by a common baryon chemical potential and chemical freeze-out temperature. The ratios indicate that the mid-rapidity region is not net baryon free, although comparison with measurements made at lower energy indicate that the net baryon density is much reduced.

Acknowledgments: Latest version of text from STAR web will be added.

REFERENCES

[1] J.-P. Blaizot, Nucl. Phys.**A 661**, 681c (1999).

[2] U. Heinz and M. Jacobs, nucl-th/00022042

[3] P. Braun-Munzinger *et al.*, hep-ph/0105229

[4] P. Koch, Z. Phys. C **38** (1988) 269.

[5] B. Müller, J. Rafelski, Phys. Rev. Lett. **48** (1982) 1066.

[6] P.Koch, B. Müller, J. Rafelski, Phys. Rep. **142** (1986) 167.

[7] NIM Paper/Conference contribution describing STAR experiment.

[8] K.H. Ackermann *et al.* (STAR Collaboration), Phys. Rev. Lett. **86** (2001) 402.

[9] S. Margetis, K. Safarik and O. Villalobos Baillie, Annu. Rev. Nucl. Sci. **50** (2000) 299-342.

[10] M. Aguilar-Benitez *et al.*, Z. Phys. **C 50** (1991) 405.

[11] Particle Data Group, Eur. Phys. J. C**3** (1998) 207.

[12] X.N. Wang, Phys. Rep. **280** (1997) 287.

[13] R. Caliandro *et al.* (WA97 Collaboration), J. Phys. G **25** (1999) 171.

[14] C. Adler *et al.* (STAR Collaboration), Phys. Rev. Lett. **86** (2001) 4478.

[15] M. Kaneta *et al.* (NA44 Collaboration), J. Phys. G **23** (1997) 1865.

[16] F. Sikler *at al.* (NA49 Collaboration), Nucl. Phys. A **661** (1999) 45c.

[17] A. Bialas, Phys. Lett. B **442** (1988) 449.

[18] J. Zimányi, T.S. Biró, T. Csörgö and P. Lévai, Phys. Lett. B **472** (2000) 243.

[19] J. Rafelski and A. Tounsi, Phys. Lett. B **292** (1992) 417.

[20] P. Braun Munzinger, I. Heppe and J. Stachel, Phys. Lett. B **465** (1999) 15.

TABLES

	K^+/K^-	$\frac{\overline{\Lambda}/\Lambda}{\overline{p}/p}$	$\frac{\overline{\Xi}^+/\Xi^-}{\overline{\Lambda}/\Lambda}$	$\sqrt{\frac{\overline{\Xi}^+/\Xi^-}{\overline{p}/p}}$
STAR	1.08 ± 0.01	1.14 ± 0.06	1.26 ± 0.08	1.19 ± 0.04
SPS	1.8 ± 0.2	1.9 ± 0.3	1.9 ± 0.6	1.9 ± 0.6

TABLE I. K^+/K^- ratio comparisons

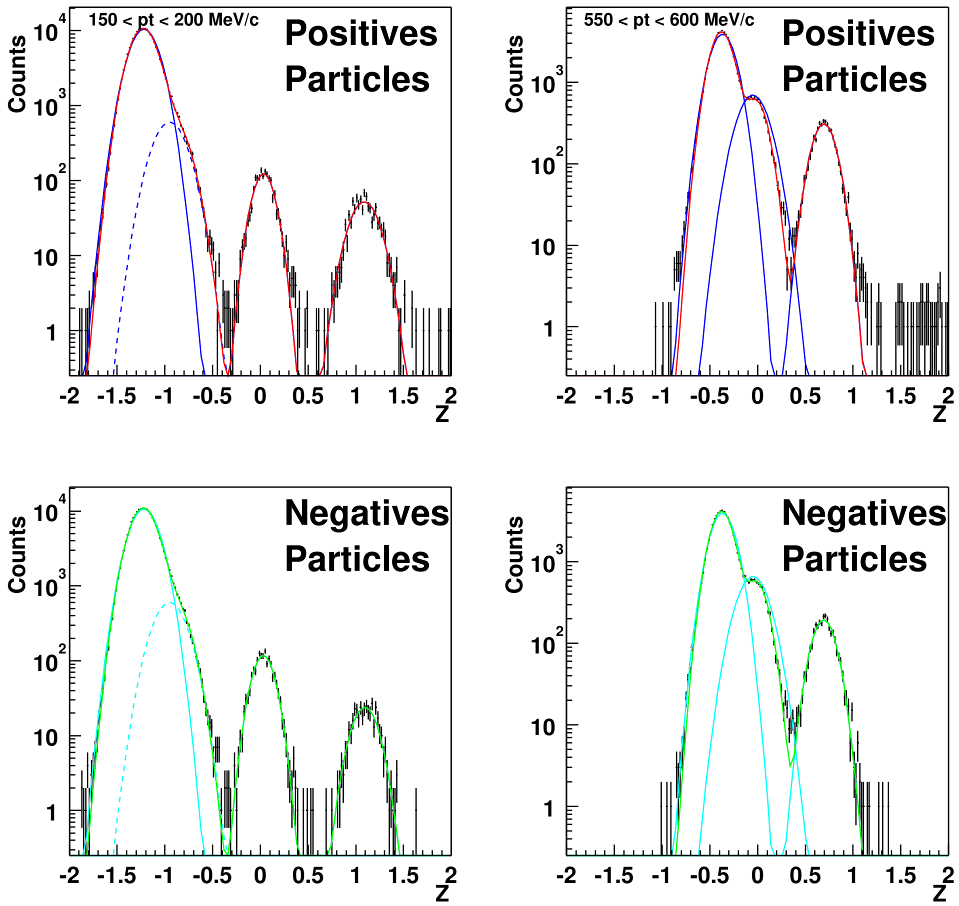

FIG. 1. Sample plots of the Z distributions for positive and negative tracks for the highest and lowest p_T bins used.

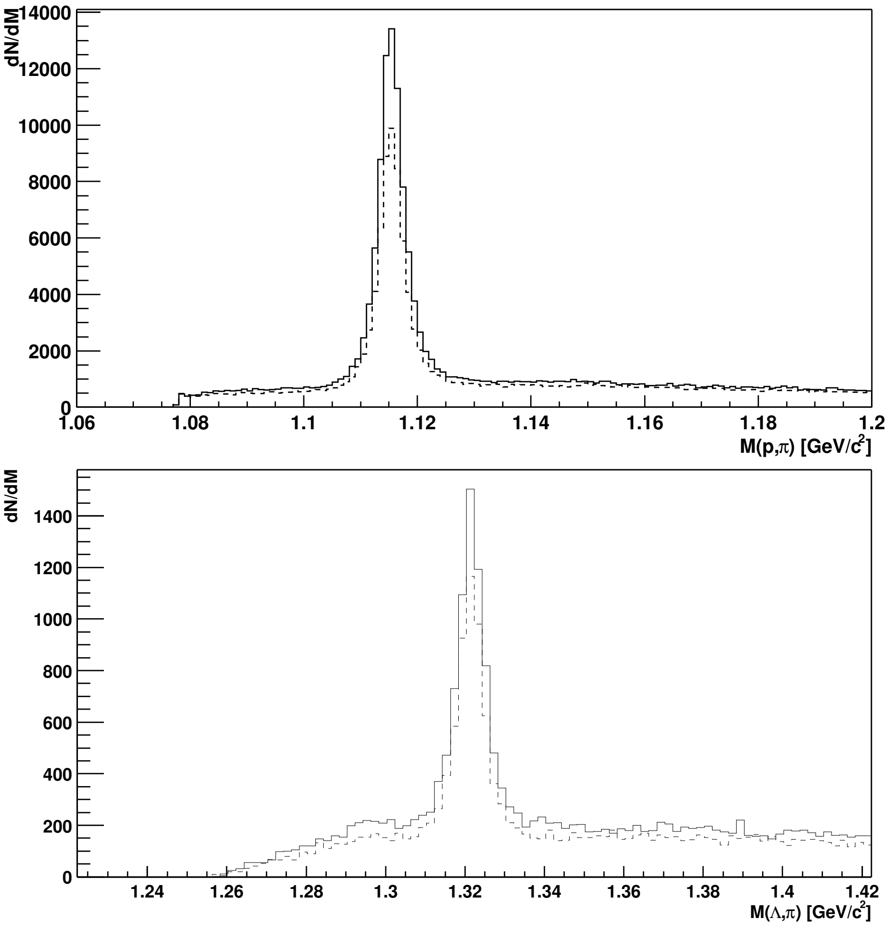

FIG. 2. Top panel. Invariant mass distributions for Λ (solid line) and $\overline{\Lambda}$ (dashed line). Lower panel. Invariant mass distributions for Ξ^- (solid line) and $\overline{\Xi}^+$ (dashed line).

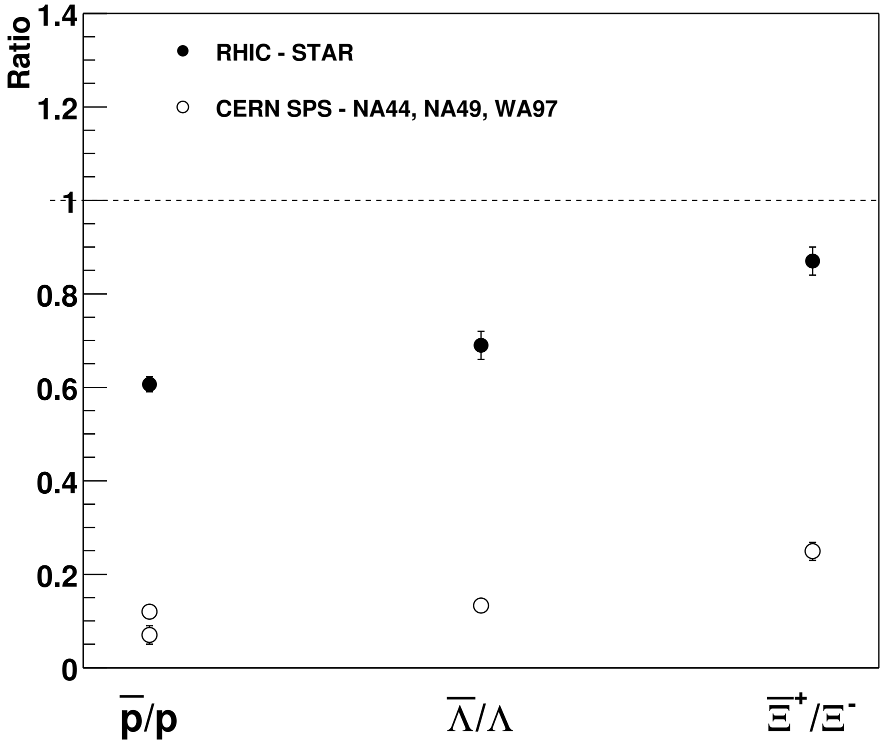

FIG. 3. Anti-baryon to baryon ratios measured by STAR, for increasingly strange baryons, compared to values obtained in experiments at the SPS [13,15,16].